AIAA Guidance, Navigation, and Control Conference and Exhibit
11-14 August 2003, Austin, Texas

AIAA 2003-5715

Experimental Validation of an Augmenting Approach to Adaptive Control of Uncertain Nonlinear Systems

Bong-Jun Yang*,
School of Aerospace Engineering, Georgia Institute of Technology
Atlanta, GA 30332
Naira Hovakimyan †,
Department of Aerospace and Ocean Engineering
Virginia Polytechnic Institute and State University
Blacksburg, VA 24061
Anthony J. Calise ‡, James I. Craig §
School of Aerospace Engineering, Georgia Institute of Technology
Atlanta, GA 30332

A method of adaptive output feedback design for uncertain nonlinear systems is presented. The development is in a form that is suitable for augmenting a linear controller. The approach is applicable to non-affine, non-minimum phase systems having parametric and dynamic uncertainties. A requirement is that the non-minimum phase zeros are represented to a sufficient accuracy in the linear controller design. The approach has been experimentally validated using a 3-disk torsional pendulum and an inverted pendulum.

Introduction

Synthesis approaches for adaptive output feedback control of uncertain nonlinear systems have a great promise for improving the performance of complex autonomous air, land, and space systems. Early results in adaptive control have been developed for very limited classes of systems, like affine in control or in uncertain parameters. Output feedback results have been developed for even more limited classes of systems, having nonlinearities depending only upon available measurement. These assumptions have been relaxed to some extent by incorporating neural networks (NNs) as an adaptive element in the synthesis approach to model the uncertainty.[1] The feasibility of applying NNs to online real-time identification and control of unknown dynamical systems has been demonstrated in several studies.[2–9]

In [10,11] two different adaptive output feedback approaches are developed for nonlinear systems, permitting the presence of unmodelled dynamics of unknown dimension. The control design layout in those approaches involves an inverting controller as a baseline design. Ref.[12] further proposed a control architecture, which augments a fixed-gain linear controller. This approach, however, employed *feedback inversion* in the adaptive part of the design, which restricts its applicability to minimum phase systems. Ref.[13] proposed a methodology which does not rely on *feedback inversion* in the adaptive design, and therefore can be applied to non-minimum phase systems.

This paper evaluates the adaptive output feedback approach proposed in Ref.[13] on laboratory models, focusing on three challenging characteristics of the control problem: modelled non-minimum phase rigid body dynamics, unmodelled flexible dynamics and nonlinear actuation.

In many applications, flexibility of the structural and mechanical elements is the main limitation on the achievable performance. Flexible systems challenge control design approaches because they introduce poorly modelled modes over a wide range of frequencies. Early applications of NN based adaptive control methods[14–17] to flexible systems were, in essence, experimental evaluation of the methods of [2–4], and lacked proofs of stability. Recently, Ref.[12] demonstrated an adaptive output feedback method that is effective in both output tracking and disturbance attenuation in a 3-disk torsional pendulum. The same laboratory model is used in validation of the current approach and is shown to achieve the same level of performance.

Adaptive control of non-minimum phase system has been challenging problem and is still an on-going research topic in both state and output feedback.[18] An inverted pendulum regulation, a typical example of a non-minimum phase control problem,[18–20] is treated

*Graduate Research Assistant, AIAA Student member, bong-jun_yang@ae.gatech.edu
†Associate Professor, nhovakimyan@vt.edu
‡Professor, AIAA Fellow, anthony.calise@ae.gatech.edu
§Professor, Senior AIAA member, james.craig@ae.gatech.edu

to illustrate the current approach.

The paper is organized as follows: After we formulate the control problem, the approach for augmenting a linear controller with an adaptive element is briefly explained. Experimental results with the torsional pendulum follow to demonstrate the validity of the approach for flexible systems. This is followed by experimental results for an inverted pendulum to show its applicability to non-minimum phase systems. Conclusions are given at the end.

Problem Formulation

Consider an *observable and stabilizable* nonlinear system in its *normal* form:[21]

$$\begin{aligned}\dot{\boldsymbol{z}}_o =& \boldsymbol{f}(\boldsymbol{z}_o, x_1, \cdots, x_r)\\ \dot{x}_1 =& x_2\\ &\vdots\\ \dot{x}_r =& h_o(\boldsymbol{z}_o, x_1, \cdots, x_r, u)\\ y =& x_1\end{aligned} \tag{1}$$

where $\boldsymbol{z}_o \in R^{n-r}$ are the states of the internal dynamics, $u \in R^1$ and $y \in R^1$ are control and measurement variables, f_o and h_o are unknown continuous functions, $f_o(0,0,0) = 0$, $h_o(0,0,0) = 0$, and r is the *strong* relative degree of the system[21] and is assumed to be known. However, n need not be known. Notice that the output y can be written as $y = \boldsymbol{c}_m^T \xi$, where

$$\begin{aligned}\xi^T \triangleq& \begin{bmatrix} x_1 & \cdots & x_r \end{bmatrix},\ \xi \in R^r\\ \boldsymbol{c}_m^T =& \begin{bmatrix} 1 & 0 & \cdots & 0 \end{bmatrix},\ \boldsymbol{c}_m \in R^r.\end{aligned} \tag{2}$$

The linear plant model, which is used to design a linear control law, is assumed to have the same relative degree r. After a suitable change of coordinates in the state space, the linear plant model can also be put in the normal form:[18]

$$\begin{aligned}\dot{\boldsymbol{z}}_l =& F_0 \boldsymbol{z}_l + \boldsymbol{g}_0 x_{l_1}\\ \dot{x}_{l_1} =& x_{l_2}\\ &\vdots\\ \dot{x}_{l_r} =& \boldsymbol{h}_0^T \boldsymbol{z}_l + a_1 x_{l_1} + \cdots + a_r x_{l_r} + bu\\ y_l =& x_{l_1}\end{aligned} \tag{3}$$

where $\boldsymbol{z}_l \in R^{m-r}$ are the states of the zero dynamics and $m \leq n$ is the dimension of the plant model.

Using the plant model in (3), the system in (1) can be written as:

$$\begin{aligned}\dot{\boldsymbol{z}}_1 =& F_0 \boldsymbol{z}_1 + \boldsymbol{g}_0 x_1 + \boldsymbol{\Delta}_2(\boldsymbol{z}_1, \boldsymbol{z}_2, \boldsymbol{\xi})\\ \dot{x}_1 =& x_2\\ &\vdots\\ \dot{x}_r =& \boldsymbol{h}_0^T \boldsymbol{z}_1 + a_1 x_1 + \cdots + a_r x_r + b[u + \Delta_1(\boldsymbol{z}_1, \boldsymbol{z}_2, \boldsymbol{\xi}, u)]\\ \dot{\boldsymbol{z}}_2 =& \boldsymbol{f}_2(\boldsymbol{z}_1, \boldsymbol{z}_2, \boldsymbol{\xi})\\ y =& x_1\end{aligned} \tag{4}$$

where $\boldsymbol{z}_o^T = [\boldsymbol{z}_1^T\ \boldsymbol{z}_2^T]$ and $\boldsymbol{z}_1 \in R^{m-r}$ represents the part of the states of the internal dynamics that are modelled through $\boldsymbol{z}_l$ in (3), and $\boldsymbol{z}_2 \in R^{n-m}$ are introduced to represent any unmodelled dynamics if $m < n$. The terms Δ_1 and $\boldsymbol{\Delta}_2$ represent the matched and unmatched uncertainties respectively, defined as:

$$\begin{aligned}\Delta_1(\boldsymbol{z}_1, \boldsymbol{z}_2, \boldsymbol{\xi}, u) =& \frac{1}{b}[h(\boldsymbol{z}_1, \boldsymbol{z}_2, \boldsymbol{\xi}, u) - \boldsymbol{h}_0^T \boldsymbol{z}_1\\ &- a_1 x_1 - \cdots - a_r x_r - bu] \qquad (5)\\ \boldsymbol{\Delta}_2(\boldsymbol{z}_1, \boldsymbol{z}_2, \boldsymbol{\xi}) =& \boldsymbol{f}_1(\boldsymbol{z}_1, \boldsymbol{z}_2, \boldsymbol{\xi}) - F_0 \boldsymbol{z}_1 - \boldsymbol{g}_0 y \qquad (6)\end{aligned}$$

Assumption 1. *The zero solution of $\dot{\boldsymbol{z}}_2 = \boldsymbol{f}_2(0, \boldsymbol{z}_2, 0)$ is globally exponentially stable, and the function $\boldsymbol{f}_2(\boldsymbol{z}_1, \boldsymbol{z}_2, \boldsymbol{\xi})$ is globally Lipschitz in its arguments.*

Consider the following output tracking controller for the dynamics in (3):

$$\begin{aligned}\dot{\boldsymbol{x}}_c =& A_c \boldsymbol{x}_c + \boldsymbol{b}_c(y_c - y)\\ u_{lc} =& \boldsymbol{c}_c^T \boldsymbol{x}_c + d_c(y_c - y)\end{aligned} \tag{7}$$

where $\boldsymbol{x}_c \in R^{n_c}$. The plant model in (3), when regulated by (7), constitutes a "reference model". Defining $\boldsymbol{\xi}_l^T \triangleq [\ x_{l_1} \quad \cdots \quad x_{l_r}\ ]$ and denoting $\boldsymbol{x}_{cl}$ the states of the controller in (7) when applied to (3), i.e. when y is replaced by y_l in (7), the "reference model" can be written as:

$$\begin{aligned}\dot{\boldsymbol{x}}_l =& \bar{A}\boldsymbol{x}_l + \bar{\boldsymbol{b}}_r y_c, \quad \boldsymbol{x}_l \in R^{m+n_c}\\ y_l =& \bar{\boldsymbol{c}}_y \boldsymbol{x}_l\end{aligned} \tag{8}$$

where $\boldsymbol{x}_l^T = [\ \boldsymbol{\xi}_l^T \quad \boldsymbol{z}_l^T \quad \boldsymbol{x}_{cl}^T\ ]$,

$$\begin{aligned}\bar{A} =& \begin{bmatrix} A_m - \boldsymbol{b}_m d_c \boldsymbol{c}_m^T & B_z & \boldsymbol{b}_m \boldsymbol{c}_c^T \\ \boldsymbol{g}_0 \boldsymbol{c}_m^T & F_0 & 0 \\ -\boldsymbol{b}_c \boldsymbol{c}_m^T & 0 & A_c \end{bmatrix},\\ \bar{\boldsymbol{b}}_r =& \begin{bmatrix} \boldsymbol{b}_m d_c \\ 0 \\ \boldsymbol{b}_c \end{bmatrix},\ \bar{\boldsymbol{c}}_y = \begin{bmatrix} \boldsymbol{c}_m \\ 0 \\ 0 \end{bmatrix},\end{aligned} \tag{9}$$

and

$$\begin{aligned}A_m =& \begin{bmatrix} 0 & 1 & 0 & \cdots \\ 0 & 0 & 1 & \cdots \\ \vdots & \vdots & \vdots & \vdots \\ a_1 & a_2 & \cdots & a_r \end{bmatrix}_{r\times r},\ B_z = \begin{bmatrix} 0 \\ 0 \\ \vdots \\ \boldsymbol{h}_0^T \end{bmatrix}_{r\times(m-r)},\\ \boldsymbol{b}_m^T =& \begin{bmatrix} 0 & 0 & \ldots & b \end{bmatrix}_{1\times r}.\end{aligned} \tag{10}$$

Note that $\bar{\boldsymbol{A}}$ is Hurwitz by design.

Let

$$u = u_{lc} - u_{ad} \tag{11}$$

When the control signal u, with u_{lc} defined in (7), is applied to the system in (4), it results in the following closed loop system:

$$\begin{aligned}\dot{\boldsymbol{x}} &= \bar{A}\boldsymbol{x} + \bar{\boldsymbol{b}}_r y_c - \bar{\boldsymbol{b}} u_{ad} + \boldsymbol{\Delta}\\ \dot{\boldsymbol{z}}_2 &= \boldsymbol{f}_2(\boldsymbol{z}_2, \boldsymbol{z}_1, \boldsymbol{\xi})\\ y &= \bar{\boldsymbol{c}}_y \boldsymbol{x}\,,\end{aligned} \tag{12}$$

in which $\boldsymbol{x}^T = [\ \boldsymbol{\xi}^T \quad \boldsymbol{z}_1^T \quad \boldsymbol{x}_c^T\ ]$, $\bar{\boldsymbol{b}}^T = [\ \boldsymbol{b}_m^T \quad 0 \quad 0\ ]$, $\boldsymbol{\Delta}^T = [\ \boldsymbol{\Delta}_1^T \quad \boldsymbol{\Delta}_2^T \quad 0\ ]$ $\boldsymbol{\Delta}_1^T = [\ 0 \quad \cdots \quad b\Delta_1\ ]$.

The objective of the control design is to augment the linear control law u_{lc} with adaptive signal u_{ad} so that the output y in (12) tracks the output y_l in (8) with bounded error, which meets design specification in tracking the reference command y_c.

Adaptive Output Feedback Augmentation

The adaptive control signal u_{ad} is designed to stabilize the error dynamics for the signal $y_l - y$. With the following definition of the error vector

$$\boldsymbol{E}^T \triangleq [\ (\boldsymbol{\xi}_l - \boldsymbol{\xi})^T \quad (\boldsymbol{z}_l - \boldsymbol{z}_1)^T \quad (\boldsymbol{x}_{cl} - \boldsymbol{x}_c)^T\ ] \quad (13)$$

comparing (8) and (12), the error dynamics can be written as:

$$\begin{aligned} \dot{\boldsymbol{E}} =& \bar{A}\boldsymbol{E} + \bar{\boldsymbol{b}}(u_{ad} - \Delta_1) - B\boldsymbol{\Delta}_2 \\ \boldsymbol{z} =& \bar{C}\boldsymbol{E}\,, \end{aligned} \quad (14)$$

where $\boldsymbol{z}$ represents the signals available for feedback:

$$\boldsymbol{z} = \begin{bmatrix} y_l - y \\ \boldsymbol{x}_{cl} - \boldsymbol{x}_c \end{bmatrix} = \underbrace{\begin{bmatrix} \boldsymbol{c}_m & 0 \\ 0 & I \end{bmatrix}}_{\bar{C}} \boldsymbol{E}\,, \quad (15)$$

and $B^T = [\ 0 \quad I \quad 0\ ]$, $I \in R^{(m-r)\times(m-r)}$. Since $\bar{A}$ is Hurwitz by design, there exist a $P = P^T > 0$ such that: for an arbitrary $Q > 0$,

$$\bar{A}^T P + P\bar{A} + Q = 0 \quad (16)$$

The control signal u_{ad} is designed to approximately cancel Δ_1. Notice from (11) and (5) that Δ_1 depends on u_{ad} through u, and that the role of u_{ad} is to cancel Δ_1. The following assumption imoposes a sufficient condition for the existence and uniqueness of a solution for u_{ad}.

Assumption 2. *The mapping $u_{ad} \mapsto \Delta_1$ is a contraction.*

Assumption 2 is equivalent to:[10]

$$\begin{aligned} sign(b) &= sign\Big(\frac{\partial h}{\partial u}\Big) \\ &\Big|\frac{\partial h}{\partial u}\Big|/2 < |b| < \infty\,. \end{aligned} \quad (17)$$

These conditions imply that control reversal is not permitted, and that there is a lower bound on the estimate of control effectiveness b.

The unmatched uncertainty $\boldsymbol{\Delta}_2$ is assumed to satisfy a *linear* bound in the error norm as in Ref.[22].

Assumption 3. $\|\boldsymbol{\Delta}_2\| \le \gamma_1 \|\boldsymbol{x}\| + \gamma_2\,, \quad \boldsymbol{x} \in \Omega_{\boldsymbol{x}} \subset R^{m+n_c}$ with known $\gamma_1, \gamma_2 > 0$.

A single hidden layer neural network(SHLNN) is used to approximate Δ_1 in (5). Since it is a function of states and control, we recall the main result from Ref.[23] which establishes a universal approximation for an unknown function of the states and control in an *observable* system using sampled values of its input/output.

Theorem 1. *For arbitrary $\epsilon^* > 0$, there exist bounded constant weights $\boldsymbol{M}, N$ such that:*

$$\Delta_1 = \boldsymbol{M}^T \boldsymbol{\sigma}(N^T \boldsymbol{\eta}) + \varepsilon(\boldsymbol{\eta}),\ \ \|\varepsilon(\boldsymbol{\eta})\| \le \epsilon^*\,, \quad (18)$$

where $\varepsilon(\boldsymbol{\eta})$ is the NN reconstruction error and $\boldsymbol{\eta}$ is the network input vector

$$\begin{aligned} \boldsymbol{\eta}(t) &= [\ 1 \quad \bar{\boldsymbol{u}}_d^T(t) \quad \bar{\boldsymbol{y}}_d^T(t)\ ]^T, \quad \|\boldsymbol{\eta}\| \le \eta^* \\ \bar{\boldsymbol{u}}_d^T(t) &= [u(t) \quad u(t-d) \quad \cdots u(t-(n_1-r-1)d)]^T \\ \bar{\boldsymbol{y}}_d^T(t) &= [y(t) \quad y(t-d) \cdots y(t-(n_1-1)d)]^T \end{aligned} \quad (19)$$

with $n_1 \ge n$ and $d > 0$, $\boldsymbol{\sigma}$ being a vector of squashing functions $\sigma(\cdot)$, its i^{th} element being defined like $\big[\boldsymbol{\sigma}(N^T\boldsymbol{\eta})\big]_i = \sigma\big[(N^T\boldsymbol{\eta})_i\big]$.

The adaptive signal u_{ad} is designed as:

$$u_{ad} = u_{nn} = \hat{\boldsymbol{M}}^T \boldsymbol{\sigma}(\hat{N}^T \boldsymbol{\eta})\,, \quad (20)$$

where $\hat{\boldsymbol{M}}$ and $\hat{N}$ are estimates of $\boldsymbol{M}$ and N to be adapted on-line. The weight adaptation laws are similar to the ones in Ref.[11] To this end, we introduce the following linear error observer for the dynamics in (14):

$$\begin{aligned} \dot{\hat{\boldsymbol{E}}} &= \bar{A}\hat{\boldsymbol{E}} + K(\boldsymbol{z} - \hat{\boldsymbol{z}}) \\ \hat{\boldsymbol{z}} &= \bar{C}\hat{\boldsymbol{E}}\,, \end{aligned} \quad (21)$$

where K is chosen to make $\bar{A} - K\bar{C}$ stable, and the following adaptive laws:

$$\begin{aligned} \dot{\hat{\boldsymbol{M}}} &= -\Gamma_M[(\hat{\boldsymbol{\sigma}} - \hat{\sigma}'\hat{N}^T\boldsymbol{\eta})\hat{\boldsymbol{E}}^T P\bar{\boldsymbol{b}} + k\hat{\boldsymbol{M}}] \\ \dot{\hat{N}} &= -\Gamma_N[\boldsymbol{\eta}\hat{\boldsymbol{E}}P\bar{\boldsymbol{b}}\hat{\boldsymbol{M}}^T\hat{\sigma}' + k\hat{N}]\,, \end{aligned} \quad (22)$$

in which $\Gamma_M, \Gamma_N > 0$ are positive definite adaptation gain matrices, $k > 0$ is a $\sigma-$modification constant, $\hat{\boldsymbol{\sigma}} \triangleq \boldsymbol{\sigma}(\hat{N}\boldsymbol{\eta})$, $\hat{\sigma}'$ is the Jacobian computed at the estimates.

In many realistic applications, it is of great interest to achieve tracking performance with the smallest possible bound. Towards this end, the control law in (11) can be augmented by an additional controller which accelerates the adaptation process and corrects NN adaptation while NN learning is at its initial phase.

Consider the following modification of the adaptive control signal u_{ad}:

$$u_{ad} = u_{nn} + u_{dc}\,, \quad (23)$$

where u_{nn} represents the previous adaptive signal defined in (20), and u_{dc} is a linear control signal, designed to robustify the error dynamics in (14) due to possible external disturbances, defined as:

$$\begin{aligned} \dot{\boldsymbol{x}}_{dc} &= A_{dc}\boldsymbol{x}_{dc} + B_{dc}\boldsymbol{z} \\ u_{dc} &= \boldsymbol{c}_{dc}^T\boldsymbol{x}_{dc} + \boldsymbol{d}_{dc}\boldsymbol{z}\,. \end{aligned} \tag{24}$$

Applying the controller in (24) to the dynamics in (14) leads to the following redefined error dynamics:

$$\dot{\boldsymbol{E}}_a = L\boldsymbol{E}_a + \begin{bmatrix} \bar{\boldsymbol{b}} \\ 0 \end{bmatrix}(u_{nn} - \Delta_1) - \begin{bmatrix} B \\ 0 \end{bmatrix}\boldsymbol{\Delta}_2\,. \tag{25}$$

where

$$\boldsymbol{E}_a = \begin{bmatrix} \boldsymbol{E} \\ \boldsymbol{x}_{dc} \end{bmatrix},\; L = \begin{bmatrix} \bar{A} + \bar{\boldsymbol{b}}\boldsymbol{d}_{dc}\bar{C} & \bar{\boldsymbol{b}}\boldsymbol{c}_{dc} \\ B_{dc}\bar{C} & A_{dc} \end{bmatrix}. \tag{26}$$

Notice that with the choice of design gains in (24), the eigenvalues of L can always be placed in the open left-half plane. The dynamics in (25) are similar to that in (14), except for the dimension of the error vector. Thus its stability analysis can be carried out similarly as in (14). The conceptual layout for the overall controller design process is presented in Figure 1.

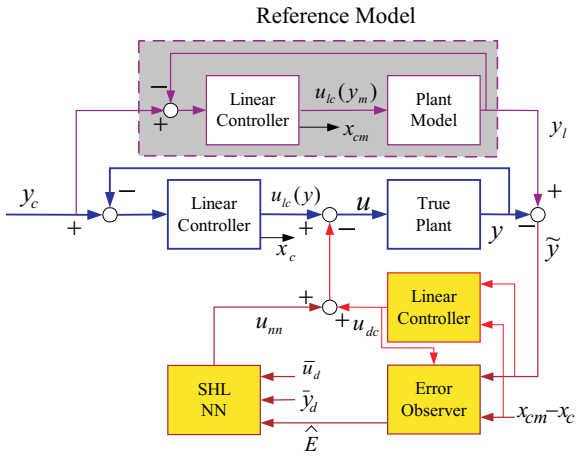

Fig. 1 Output Feedback Augmentation Architecture

Experimental Results with a 3-disk Torsional Pendulum System

Figure 2 depicts a torsional pendulum system which is made up of three disks connected by a flexible shaft.[24] Only the bottom disk(θ_3) is actuated by a brushless DC servo motor. The equations of motion for the system are as follows:

$$\begin{aligned} &J_1\ddot{\theta}_1 + B\dot{\theta}_1 + K(\theta_1 - \theta_2) + f_{c_1}(\dot{\theta}_1, \theta_1, \theta_2) = K_dV_d \\ &J_2\ddot{\theta}_2 + B\dot{\theta}_2 - K\theta_1 + 2K\theta_2 - K\theta_3 + f_{c_2}(\dot{\theta}_2, \theta_1, \theta_2, \theta_3) = 0 \\ &J_3\ddot{\theta}_3 + B\dot{\theta}_3 - K(\theta_2 - \theta_3) + f_{c_3}(\dot{\theta}_3, \theta_2, \theta_3) = K_{vt}u \end{aligned} \tag{27}$$

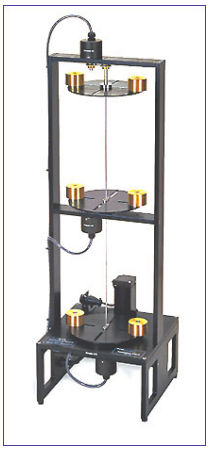

Fig. 2 The 3-disk Torsional Pendulum System.[24]

where $J_i = 0.103kg{\cdot}m^2,\ i = 1,2,3$ are the moments of inertia, $B = 0.0018kg\cdot m/s$ is the viscous damping coefficient, $K = 2.2625kg\cdot m^2/s^2$ is the spring constant, $K_d = 0.05\frac{N\cdot m}{V}$ is the gain from disturbance voltage to torque, $K_{vt} = 0.42\frac{N\cdot m}{V}$ is the gain from control voltage to torque, and f_{c_i} represents nonlinearities, such as coulomb friction. The control input u is the applied voltage to the control motor and the disturbance input V_d is the applied voltage to the disturbance drive.

Bottom Disk Control - a Collocated Control Problem

When the regulated output variable is the angular displacement of the bottom disk θ_3, the output variable is *collocated* with the control u. The output has relative degree 2 if the dynamics of the DC motor are treated as lying outside the bandwidth of the design. With $f_{c_i} = 0$, the transfer function from applied voltage to the regulated output is given by the 6th order model:

$$\frac{\theta_3}{u} = \frac{K_a(s^2 + 2\zeta_{z_1}\omega_{z_1}s + \omega_{z_1}^2)(s^2 + 2\zeta_{z_2}\omega_{z_2}s + \omega_{z_2}^2)}{s(s+c)(s^2 + 2\zeta_{p_1}\omega_{p_1}s + \omega_{p_1}^2)(s^2 + 2\zeta_{p_2}\omega_{p_2}s + \omega_{p_2}^2)} \tag{28}$$

The parameters were determined experimentally to be: $K_a = 40.46$, $\zeta_{z_1} = 0.009$, $\omega_{z_1} = 9.87$, $\zeta_{z_2} = 0.0035$, $\omega_{z_2} = 25.8$, $c = 0.1786$, $\zeta_{p_1} = 0.00559$, $\omega_{p_1} = 16(rad/sec)$ and $\zeta_{p_2} = 0.00323$, $\omega_{p_2} = 27.7(rad/sec)$. The zero dynamics for the system in (27), with $f_{c_i} = 0$, are given by:

$$\begin{aligned} &J_1\ddot{\theta}_1 + B\dot{\theta}_1 + K(\theta_1 - \theta_2) = K_dV_d \\ &J_2\ddot{\theta}_2 + B\dot{\theta}_2 - K\theta_1 + 2K\theta_2 = 0 \\ &\dot{\boldsymbol{x}}_d = f_d(\boldsymbol{x}_d) \\ &V_d = h_d(\boldsymbol{x}_d) \end{aligned} \tag{29}$$

where $\boldsymbol{x}_d$ represents the states of the *bounded* disturbance dynamics. The eigenvalues associated with the zero dynamics are $-0.089\pm15.97i$ and $-0.893\pm27.66i$. Therefore the system is minimum phase.

To emphasize the presence of unmodelled dynamics, the following low frequency model for the plant

dynamics, that does not include the flexible modes, is used for the control design:

$$\frac{y}{u} = \frac{K}{s(s+c)} \tag{30}$$

where $K = 13.49, c = 0.18$ is determined such that low frequency gain of the plant model matches that of the linear 6th order plant given in (28). Since the plant model in (30) does not have zero dynamics, the zero dynamics in (29) represents unmodelled dynamics. The matrices for plant model in its normal form are as follows:

$$A_m = \begin{bmatrix} 0 & 1 \\ 0 & -0.18 \end{bmatrix}, \ \boldsymbol{b}_m = \begin{bmatrix} 0 \\ 13.49 \end{bmatrix}, \ \boldsymbol{c}_m = \begin{bmatrix} 1 \\ 0 \end{bmatrix} \tag{31}$$

Figure 3 compares the frequency response of the assumed plant model with that of the linear 6th order model. The agreement is quite good at low frequencies but differs significantly at high frequencies due to the unmodelled flexible modes.

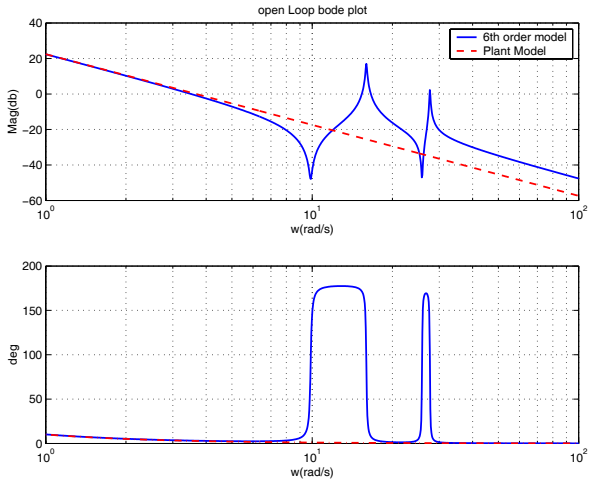

Fig. 3 The Open Loop Bode Plot for the 6th Order Model and the Plant Model for the Bottom Disk.

The linear controller is designed as a lead compensator, which results in a dominant mode at $\omega_n = 3rad/s$ and $\zeta = 0.8$ for the nominal system design. This resulted in:

$$u_{lc} = K_1 \frac{s+b_1}{s+a_1}(y_c - y) \tag{32}$$

where $K_1 = 0.67, a_1 = 4.8, b_1 = 0.1786$.

Equation (21) represents a full order observer. Define $\boldsymbol{e}^T = [y_l - y, \ \dot{y}_l - \dot{y}]$. Since the states of the controller are available, we design a reduced order observer to obtain an estimate for e_2:

$$\dot{\hat{\boldsymbol{e}}} = A_m \hat{\boldsymbol{e}} + \boldsymbol{b}_m[u_{lc}(y_m) - u_{lc}(y)] + \boldsymbol{b}_m u_{dc} + K(e_1 - \hat{e}_1) \tag{33}$$

where $u_{lc}(y_m)$ is the linear control signal in the reference model and $u_{lc}(y)$ is the linear control signal in the system, as they are depicted in Figure 1. The observer gain K is decided so that the eigenvalues of $A_m - K\boldsymbol{c}_m^T$ are $-46.2 \pm 46.2i$. Then the error vector as in (21) is constructed as:

$$\hat{\boldsymbol{E}} = \begin{bmatrix} \hat{\boldsymbol{e}} \\ x_{cl} - x_c \end{bmatrix} \tag{34}$$

A SHLNN is introduced to approximate the uncertainty Δ_1. It has 5 hidden layers, with 5 delayed values of y for $\bar{\boldsymbol{y}}_d$ combined with 3 delayed values of u for $\bar{\boldsymbol{u}}_d$ as its input vector, and has the following learning rates and $\sigma-$modification factor:

$$\Gamma_M = 0.5I, \ \Gamma_N = 0.5I, \ k = 1.3$$

The additional control u_{dc} is added to accelerate NN adaptation. It is designed as a linear quadratic Gaussian(LQG) controller so as to attenuate the disturbance, NN reconstruction error $u_{nn} - \Delta_1$ in (14).

In the first experiment, the performance of output tracking with and without the proposed adaptive element is compared when a square wave command of 20° with 20 Hz is applied. Figure 4 compares the response of the regulated output. The response without the adaptive element is shown dash-dotted and the output of the reference model in (8) is dashed. The absence of the flexible modes in the response with the adaptive element shows that the augmented controller provides adaptation to the unmodelled flexible modes. Furthermore, the output response without the adaptive element resulted in a large steady state error. This is caused by coulomb friction. The effect of coulomb friction, which corresponds to f_{c_3} in (27), are not modelled in the linear controller design. The output response with the adaptive element shows almost perfect tracking for y_l.

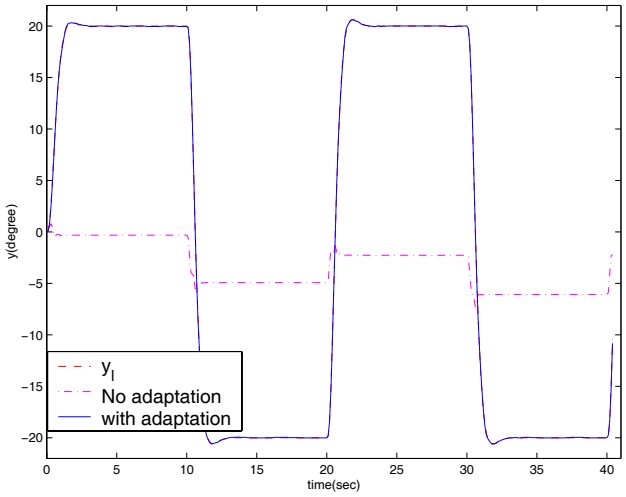

Fig. 4 Comparison of the Output Response of the Bottom Disk with and without the Adaptive Element

In the second set of experiments, disturbance attenuation is evaluated with $y_c = 0$. A disturbance was introduced using a friction drive motor attached to the

rim of the top disk. Note that the disturbance is not collocated with the control. The disturbance is made up of sinusoids:

$$\begin{aligned} V_d(t) =& 0.5\sin t + 0.3\sin 2t + 0.2\sin 10t \\ &+ 0.2\sin 15.7t + 0.2\sin 27.7t \end{aligned} \tag{35}$$

The output responses of the open loop plant, the plant controlled without the adaptive element, and the plant controlled with the adaptive element are compared in Figure 5. The response of the open loop system is shown dotted, the output of the system regulated only by the linear controller is dash-dotted, and the output of the system with the adaptive element is solid. Note that the linear controller does provide a level

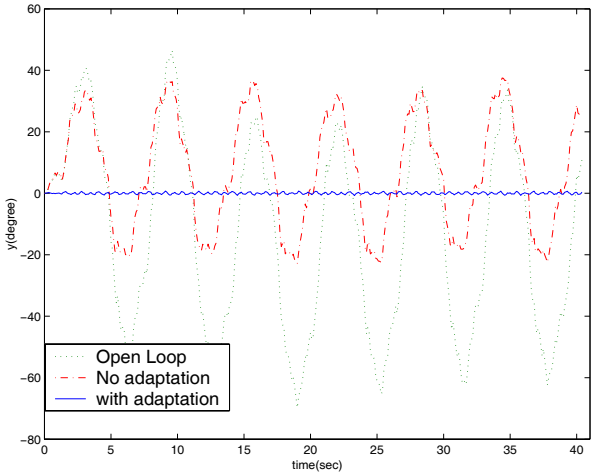

Fig. 5 Output response of the Bottom Disk under Sinusoidal Disturbances

of response reduction in comparison to the open loop response. When the adaptive element is added to the linear controller, the response is nearly reduced to zero. This result is analogous to the experimental results presented in Ref.[12].

Middle Disk Control - a Non-collocated Control Problem

When the regulated output variable is the angular displacement of the middle disk θ_2, the output variable is *non-collocated* with the control u. The output has relative degree 4. To ensure observability of the system, two more masses are added on the bottom disk, resulting in the moments of inertia for the system in (27) as $J_1 = J_2 = 0.0078, J_3 = 0.0138$. The transfer function from u to θ_2 is as follows:

$$\frac{\theta_2}{u} = \frac{K_a(s^2 + 2\zeta_{z_1}\omega_{z_1}s + \omega_{z_1}^2)}{s(s+c)(s^2 + 2\zeta_{p_1}\omega_{p_1}s + \omega_{p_1}^2)(s^2 + 2\zeta_{p_2}\omega_{p_2}s + \omega_{p_2}^2)} \tag{36}$$

The parameters are : $K_a = 10170$, $\zeta_{z_1} = 0.0064$, $\omega_{z_1} = 18.4$, $c = 0.1877$, $\zeta_{p_1} = 0.0059$, $\omega_{p_1} = 16(rad/sec)$ and $\zeta_{p_2} = 0.0037$, $\omega_{p_2} = 30.7(rad/sec)$. The zero dynamics , similarly as in (29), are given by:

$$\begin{aligned} &J_1\ddot{\theta}_1 + B\dot{\theta}_1 + K(\theta_1 - \theta_2) = K_d V_d \\ &\dot{\boldsymbol{x}}_d = f_d(\boldsymbol{x}_d) \\ &V_d = h_d(\boldsymbol{x}_d) \end{aligned} \tag{37}$$

The associated eigenvalues are $-0.089 \pm 15.97i$. Therefore it is minimum phase.

In the plant model, the shaft which connects the top and middle disk is assumed rigid. Furthermore, it is assumed that the moments of inertia in (27) are of the same value, i.e.,$J_i = 0.103$ $i = 1, 2, 3$, which results in the following transfer function:

$$\frac{\theta_2}{u} = \frac{K}{s(s+c)(s^2 + 2\zeta_n\omega_n s + \omega_n^2)} \tag{38}$$

where $K = 5159$, $c = 0.18$, $\zeta_n = 0.0046$, $\omega_n = 19.6$. The plant model in (38) does not have zero dynamics as in (30). With the states defined as $\boldsymbol{s}_l = [\theta_2, \dot{\theta}_2, \theta_3, \dot{\theta}_3]$, the matrices for plant model in its state space form are as follows:

$$\begin{aligned} A_m &= \begin{bmatrix} 0 & 1 & 0 & 0 \\ -127.5 & -0.1786 & 127.5 & 0 \\ 0 & 0 & 0 & 1 \\ 255 & 0 & -255 & -0.1786 \end{bmatrix}, \\ \boldsymbol{b}_m &= \begin{bmatrix} 0 \\ 0 \\ 0 \\ 40.47 \end{bmatrix}, \quad \boldsymbol{c}_m = \begin{bmatrix} 1 \\ 0 \\ 0 \\ 0 \end{bmatrix} \end{aligned} \tag{39}$$

Figure 6 compares the frequency response of the assumed plant model with that of the linear 6th order model in (36).

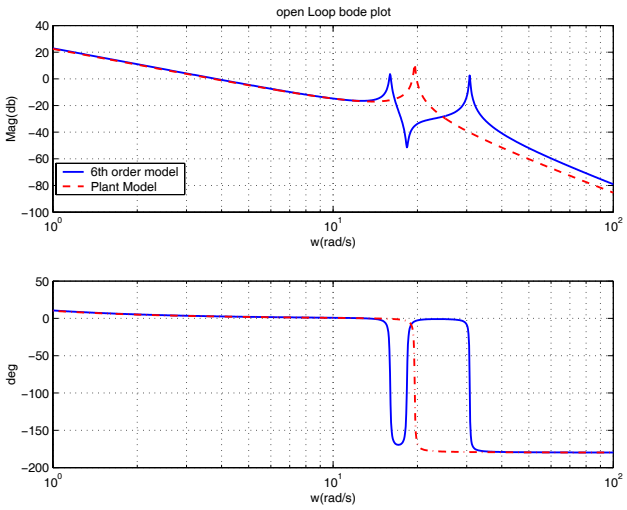

Fig. 6 The Open Loop Bode Plot for the 6th Order Model and the Plant Model for the Middle Disk.

The linear controller in (7) is designed as a LQG

controller:

$$A_c = \begin{bmatrix} -1.5 & 1 & 0 & 0 \\ -128.7 & -0.2 & 128.7 & 0 \\ -1.5 & 0 & 0 & 1 \\ 992.6 & -22.8 & -1016.9 & -133.8 \end{bmatrix},$$
$$\boldsymbol{b}_c = \begin{bmatrix} -1.55 \\ -1.20 \\ -1.54 \\ -1.19 \end{bmatrix}, \quad \boldsymbol{c}_c = \begin{bmatrix} -18.26 \\ 0.56 \\ 18.83 \\ 3.30 \end{bmatrix}, \quad d_c = 0 \tag{40}$$

The reduced error observer is designed, after transforming the system in (39) into its normal form, similarly as in (33) with the following definition for $\boldsymbol{e}^T = [y_l - y, \dot{y}_l - \dot{y}, \ldots, y_1^{(3)} - y^{(3)}]$. The observer gain K is decided so that the eigenvalues of $A_m - K\boldsymbol{c}_m^T$ are $-182.3 \pm 440.5i, -440.1 \pm 182.5i$. The SHLNN and the additional control signal u_{dc} are designed in the similar manner as in the bottom disk control problem.

Figure 7 compares output responses with and without the adaptive element when the same square wave as in the bottom disk control is applied. It is notable that the linear controller without the adaptive element almost completely fails to overcome the stiction due to increased inertia which is not captured in the plant model. Compared to perfect tracking shown in Figure 4, the response with the adaptive element is more oscillatory. The steady state error is, however, effectively eliminated. Figure 8 compares the output responses,

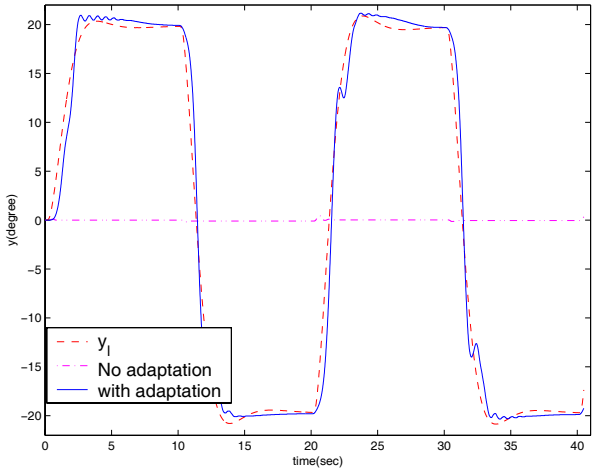

Fig. 7 Comparison of the Output Response of the Middle Disk with and without the Adaptive Element

when the same disturbance as in (35) is applied. The control law with adaptation shows significant disturbance rejection compared to that of the linear control law without the adaptive element. However, the disturbance attenuation is not as drastic as Figure 5.

Experimental Results with an Inverted Pendulum

Figure 9 depicts an inverted pendulum mechanism, Quanser Inc.[25] It consists of a motor driven cart,

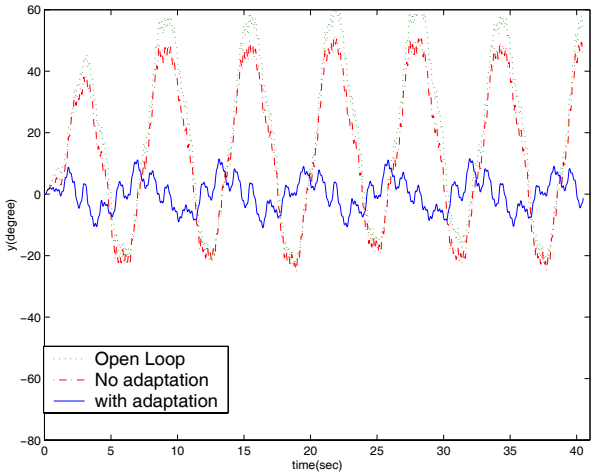

Fig. 8 Output Response of the Middle Disk under Sinusoidal Disturbances

which is equipped with two quadrature encoders. One encoder (0.05mm resolution) measures the position of the cart via a pinion (x), which meshes with the track. The other encoder(0.09° resolution) measures the angle of the pendulum(θ), which is free to swing at the side of the cart. The equations of motion for the sys-

Fig. 9 The inverted pendulum.[25]

tem are as follows:

$$\begin{aligned} &(M+m)\ddot{x} + c_M\dot{x} + ml_p\ddot{\theta}\cos\theta - ml_p\dot{\theta}^2\sin\theta + \Psi(\dot{x},x) = F \\ &ml_p\cos\theta\ddot{x} + (J_p + ml_p^2)\ddot{\theta} + c_m\dot{\theta} - mgl_p\sin\theta = 0 \end{aligned} \tag{41}$$

where x is the displacement of the cart along the track (m), F is the force applied to the cart (N), M is the mass of the cart(kg), m is the mass of the rod(kg), l_p is the position of the center of gravity of the rod (half of full length)(m), $J_p = \frac{1}{3}ml_p^2$ is a moment of inertia of the rod with respect to its center of gravity($kg \cdot m^2$), g is the gravitational acceleration ($kg \cdot m/sec^2$), c_M, c_m are the viscous damping coefficients, and $\Psi(\dot{x},x)$ is an uncertain nonlinearity which is caused by the cart moving mechanism, i.e., combined effects of stiction,

coulomb friction, and backlash. There are also unmodelled dynamics due to flexibility in the direction perpendicular to the track. The force, F, is a consequence of an input voltage u applied to a DC motor and the cart velocity, according to the following equations:

$$F = \frac{K_m K_g}{R_m r} u - \frac{K_m^2 K_g^2}{R_m r^2} \dot{x} = a_1 u - a_2 \dot{x} \tag{42}$$

where K_m is a back EMF constant(Volts/(rad/sec)), K_g is a gear ratio in motor gearbox, R_m is a motor armature resistance (Ohms), and r is the radius of motor pinion that meshes with the track (m). The system parameters are: $M = .815,\ m = 0.21,\ l_p = 0.305,\ g = 9.8,\ a_1 = 2.33,\ a_2 = 10.42$. The control objective is to regulate x so that it tracks the reference command y_c, using measured outputs $x,\ \theta$ while balancing the inverted pendulum.

With the definition, $x_1 = x, x_2 = \dot{x}, z_1 = \theta, z_2 = \frac{\dot{x}}{l_p}\cos\theta + \frac{4}{3}\dot{\theta}$, the system in (41) is put into a normal form:

$$\begin{aligned}
\dot{x}_1 &= x_2 \\
\dot{x}_2 &= \frac{1}{M + m(1 - 3/4\cos\theta^2)}\big[\, a_1 u - a_2 x_2 \\
&\quad - c_M x_2 - \Psi(x_1, x_2) + m l_p \dot{\theta}^2 \sin\theta \\
&\quad + \frac{3}{4} c_m \dot{\theta}\cos\theta - \frac{3}{4} mg \sin\theta\cos\theta \,\big] \\
\dot{z}_1 &= \frac{3}{4} z_2 - \frac{3\cos\theta}{4 l_p} x_2 \\
\dot{z}_2 &= \frac{g}{l_p}\sin\theta - \frac{c_m}{m l_p}\dot{\theta} - \frac{1}{l_p} x_2 \dot{\theta}\sin\theta
\end{aligned} \tag{43}$$

Its zero dynamics are given by:

$$\begin{aligned}
\dot{z}_1 &= \frac{3}{4} z_2 \\
\dot{z}_2 &= \frac{g}{l_p}\sin z_1 - \frac{3 c_m}{4 m l_p} z_2.
\end{aligned} \tag{44}$$

Linearization of z_1, z_2 dynamics in (44) about the desired equilibrium point $(z_1, z_2) = (0, 0)$, reveals an eigenvalue at $\frac{c_m}{m l_p}\left[-\frac{3}{8} + \frac{1}{2}\sqrt{1 + \frac{3 m^2 g l_p}{c_m^2}}\right] > 0$. Therefore the system is non-minimum phase.

The plant model is constructed linearizing Eq.(41) with $J_p = 0$. Furthermore, the uncertain nonlinearity $\Psi(\dot{x}, x)$ and viscous damping terms (c_M, c_m) are not accounted in the linear model. With $x_{l_1} = x,\ x_{l_2} = \dot{x},\ z_{l_1} = \theta,\ z_{l_2} = \frac{\dot{x}}{l_p} + \dot{\theta}$, it is put into the following normal form:

$$\begin{aligned}
\dot{x}_{l_1} &= x_{l_2} \\
\dot{x}_{l_2} &= \frac{1}{M}[a_1 u - a_2 x_{l_2} - mg\theta] \\
\dot{z}_{l_1} &= z_{l_2} - \frac{1}{l_p} x_{l_2} \\
\dot{z}_{l_2} &= \frac{g}{l_p}\theta
\end{aligned} \tag{45}$$

Comparing (45) with (43) leads to the following matched and unmatched uncertainties.

$$\begin{aligned}
\Delta_1 &= \frac{1}{a_1}\Big[\frac{M}{M + m(1 - 3/4\cos\theta^2)}\big[a_1 u - a_2 x_2 \\
&\quad - c_M x_2 - \Psi(x_1, x_2) + m l_p \dot{\theta}^2 \sin\theta + \frac{3}{4} c_m \dot{\theta}\cos\theta \\
&\quad - \frac{3}{4} mg \sin\theta\cos\theta\big] + mg\theta - a_1 u + a_2 x_2\Big] \\
\boldsymbol{\Delta}_2 &= \begin{bmatrix} -\frac{1}{4} z_2 + \frac{1}{l_p} x_2 (1 - \frac{3}{4}\cos\theta) \\ \frac{g}{l_p}(\sin\theta - \theta) - \frac{c_m}{m l_p}\dot{\theta} - \frac{1}{l_p} x_2 \dot{\theta}\sin\theta \end{bmatrix}
\end{aligned} \tag{46}$$

The linear controller is designed as a LQG controller based on the plant model in (45), in which two measured outputs $x_1,\ z_1(=\theta)$ are available. In the experimental tests, it was observed that a high bandwidth design is stabilizing, while a low bandwidth design results in an unstable system. To address the effectiveness of the approach, we augmented the low bandwidth design. The LQG controller places the eigenvalues of $\bar{A}$ at $-0.3, -4.9 \pm 1.3i, -8.2 \pm 5.9i, -10.3 \pm 2.4, -31.6$.

The reduced order error observer in (33) was designed so that its poles are located at $-1.0, -99.9, -26.5 \pm 24.0i$. The additional controller is not necessary, so $u_{dc} = 0$. Since two outputs are available, network inputs are constructed as follows:

$$\boldsymbol{\eta}^T = [x_1,\ x_1(t-d),\ z_1,\ z_1(t-d), u],\ d = 0.01 sec.$$

The NN consists of 6 neurons in the hidden layer and its parameters are:

$$\Gamma_M = 150I,\ \Gamma_N = 150I,\ k = 1.2. \tag{47}$$

Figures 10 and 11 show the experimental results with $y_c = 0$. The pendulum is swung up to the vertical position by hand before the the proposed controller starts at t=7.8 sec. While the linear controller is augmented by the adaptive NN, the cart position and the angle of the pendulum are regulated within $\pm 0.05(m)$

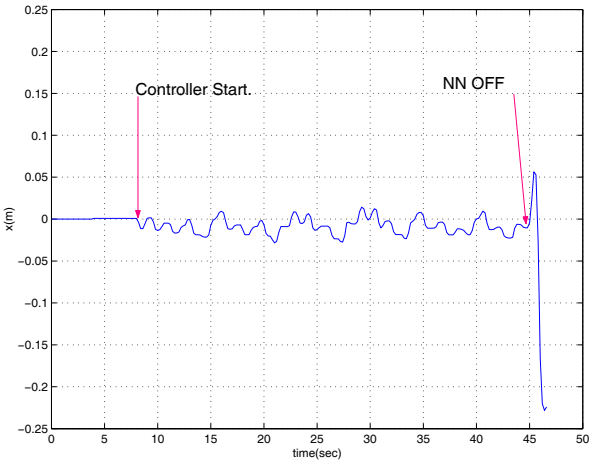

Fig. 10 The Cart Position (m) with $y_c = 0$.

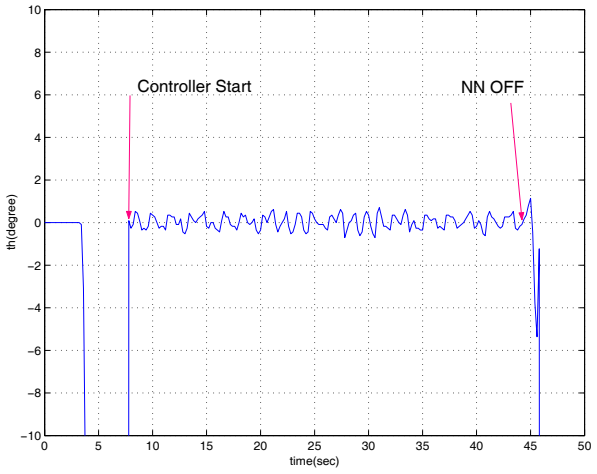

Fig. 11 The Angle(degree) of the Pendulum with $y_c = 0$.

and $\pm 1°$. When the NN is turned off at t=44.6 sec., the control system immediately goes unstable.

Figures 12 and 13 show the output responses when a square wave command of 0.15 m with 0.01 Hz is applied. The result shows that y_l is tracked with a bounded error, while the inverted pendulum being quickly stabilized after a short transient.

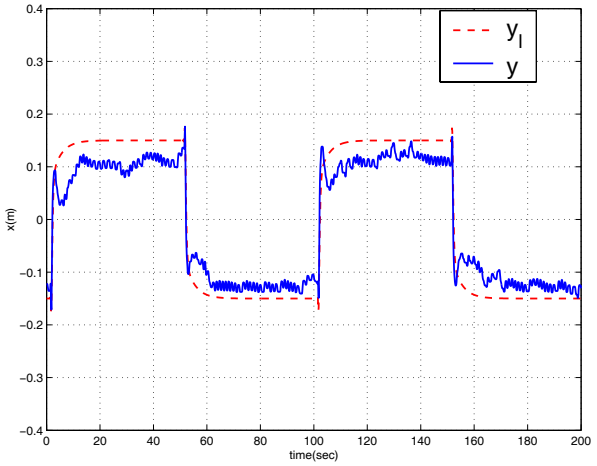

Fig. 12 The Cart Position(m) with y_c of a Square Wave Command.

Conclusions

This paper describes and evaluates an approach for augmenting a linear controller with an adaptive element that can be applied to both minimum phase and non-minimum phase uncertain nonlinear systems. The linear controller can either be an existing controller or a controller that is explicitly designed as a part of the overall adaptive controller architecture. The key properties of the design are that only output variables are used, and it is adaptive to both parametric errors and unmodelled/unmatched dynamics and disturbances. The main assumptions are that the relative degree of the regulated output is known, and that the

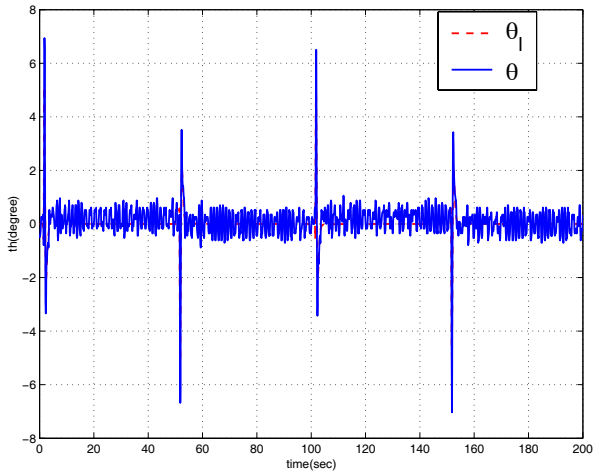

Fig. 13 The Angle(degree) of the Pendulum with y_c of a Square Wave Command.

unmatched uncertainty in the error dynamics satisfies a conic sector bound. In the case of non-minimum phase zero dynamics, the non-minimum phase zeros must be accounted for in the design of the linear controller to sufficient accuracy.

Experimental results obtained using a 3-disk torsional pendulum laboratory model, which is minimum phase, shows that the proposed control law achieves significant improvement in tracking and disturbance attenuation. Experimental results with an inverted pendulum further illustrate the effectiveness of the approach for control of a non-minimum phase nonlinear system.

References

[1]Hornik, N., Stinchcombe, M., and White, H., "Multilayer feedforward networks are universal approximators," *Neural Networks*, Vol. 2, 1989, pp. 359–366.

[2]Narendra, K. and Parthasarathy, K., "Identification and control of dynamical systems using neural networks," *IEEE Transactions on Neural Networks*, Vol. 1, Mar. 1990, pp. 4–27.

[3]Narendra, K., "Adaptive Control of Dynamical Systems Using Neural Networks," *Handbook of Intelligent Control*, edited by D. A. White and D. A. Sofge, Van Nostrand Reinhold, New York, 1992.

[4]Narendra, K., "Neural Networks for Control: Theory and Practice," *Proceedings of the IEEE*, Vol. 84, No. 10, Oct. 1996, pp. 1385–1996.

[5]Lewis, F., Jagannathan, S., and Yeşildirek, A., *Neural Network Control of Robot Manipulators and Nonlinear Systems*, Taylor & Francis, 1999.

[6]Polycarpou, M., "Stable Adaptive Neural Control Scheme for Nonlinear Systems," *IEEE Transactions on Automatic Control*, Vol. 41, No. 3, 1996, pp. 447–451.

[7]Ge, S., Lee, T., and Harris, C., *Adaptive Neural Network Control of Robotic Manipulators*, World Scientific, 1998.

[8]Rovithakis, G., "Robustifying Nonlinear Systems Using High-Order Neural Network Controller," *IEEE Transactions on Automatic Control*, Vol. 44, 1999, pp. 102–108.

[9]Calise, A., Lee, S., and Sharma, M., "Development of a Reconfigurable Flight Control Law for Tailless Aircraft," *AIAA Journal of Guidance,Control and Dynamics*, Vol. 24, No. 5, 2001, pp. 896–902.

[10]Calise, A., Hovakimyan, N., and Idan, M., "Adaptive Output Feedback Control of Nonlinear Systems using Neural Networks," *Automatica*, Vol. 37, 2001, pp. 1201–1211.

[11]Hovakimyan, N., Nardi, F., Kim, N., and Calise, A., "Adaptive Output Feedback Control of Uncertain Systems using Single Hidden Layer Neural Networks," *IEEE Transactions on Neural Networks*, Vol. 13, No. 6, 2002.

[12]Calise, A., Yang, B.-J., and Craig, J., "An Augmenting Adaptive Approach to Control of Flexible Systems," *Proceedings of AIAA guidance,navigation and control conference*, 2002.

[13]Hovakimyan, N., Yang, B.-J., and Calise, A., "An Adaptive Output Feedback Control Methodology for Non-Minimum Phase Systems," *Proceedings of Conference on Decision and Control*, Las Vegas, NV, 2002, pp. 949–954.

[14]Rao, V., Damle, R., Tebbe, C., , and Kern, F., "The adaptive control of smart structures using neural networks," *Smart Materials and Structures*, Vol. 3, 1994, pp. 354–366.

[15]Hyland, D. C., "Neural Network Architecture for On-Line System Identification and Adaptively Optimized Control," *Proceedings of the Conference on Decision and Control*, Brighton, England, Dec. 1991, pp. 2552–2557.

[16]Hyland, D. C., "Adaptive Neural Control for Flexible Aerospace Systems: Progress and Prospects," *10th IEEE International Symposium on Intelligent Control*, 1995, pp. 3–8.

[17]KrishnaKumar, K. and Montgomery, L., "Adaptive neurocontrol for large flexible structures," *Smart Materials and Structures*, Vol. 1, 1992, pp. 312–323.

[18]Isidori, A., "A Tool for Semiglobal Stabilization of Uncertain Non-Minimum-Phase Nonlinear Systems via Output Feedback," *IEEE Transactions on Automatic Control*, Vol. 45, No. 10, 2000, pp. 1817–1827.

[19]Huang, J., "Asymptotic Tracking of a Nonminimum Phase Nonlinear System with Nonhyperbolic Zero Dynamics," *IEEE Transactions on Automatic Control*, Vol. 45, No. 3, 2000, pp. 542–546.

[20]Atassi, A. and Khalil, H., "A Separation Principle for the Stabilization of a Class of Nonlinear Systems," *IEEE Transactions on Automatic Control*, Vol. 44, No. 9, Sep. 1999, pp. 1672–1687.

[21]Sastry, S., *Nonlinear Systems*, Springer-Verlag, 1999.

[22]Chen, Y., "Design of Robust Controllers for Uncertain Dynamical Systems," *IEEE Transactionson Automatic Control*, Vol. 33, No. 5, 1988, pp. 487–491.

[23]Lavretsky, E., Hovakimyan, N., and Calise, A., "Reconstruction of Continuous-Time Dynamics Using Delayed Outputs and Feedforward Neural Networks," *IEEE Transactions on Automatic Control*, 2003, to appear in Sept.

[24]"Torsion Pendulum Appratus, ECP Systems, Inc." `http://www.ecpsystems.com/controls/torplant.htm`.

[25]"Inverted Pendulum, Quanser Inc." `http://www.quanser.com/english/html/challenges/fs\_chall\_linear\_flash.htm`.